FEM ANALYSIS OF RIVETED CONNECTIONS AIMING FATIGUE AND FRACTURE ASSESSMENTS

A.M.P de Jesus[1,2] , R. M. G. Pereira [1,2]

[1] Departamento de Engenharias, Escola de Ciências e Tecnologia,
Universidade de Trás-os-Montes e Alto Douro, Quinta de Prados,
5001-801 Vila Real, Portugal.
E-mail: ajesus@utad.pt; rmmurca@hotmail.com

[2] Unidade de Concepção e Validação Experimental,
Instituto de Engenharia Mecânica – IDMEC, Pólo FEUP
Rua Dr. Roberto Frias, 4200-465 Porto, Portugal

ABSTRACT

Old riveted bridges are susceptible to exhibit significant fatigue damage levels, since they were originally designed without taking into account the fatigue phenomenon and they were subjected to increasing loading, along their long operational period. Due to economic reasons, the operational period of those structures has been further increased, requiring detailed residual fatigue life studies. The usual procedures for fatigue analysis of riveted connections are based on the S-N approach. The local approaches and Fracture Mechanics appear as alternatives to the S-N approach, to derive the fatigue strength for riveted joints, with higher flexibility than S-N approaches. These alternative approaches require detailed stress analysis. This paper proposes a methodology for detailed stress analysis of multi-riveted connections using the Finite Element Method. The proposed methodology is demonstrated for a stringer-to-cross-girder intersection, using the ANSYS® commercial code. This methodology consists on 3D finite element models using both solid and shell elements as well as contact elements. The proposed model is able to account the clamping stresses of rivets on stress distributions. Also, choosing several crack propagation scenarios, the stress intensity factors are evaluated using the crack closure technique.

KEY WORDS: riveted connections, finite element analysis, stress analysis, fracture mechanics.

1. INTRODUCTION

Structural integrity assessments of old steel riveted bridges are more and more frequent. Most of these structures were built at the end of the 19th century or the beginning of the 20th century with angles and plates joined by rivets and made of puddle iron or wrought steel. Fatigue is one major concern for these structures since they show a long operational period with increasing traffic intensity, many times without the required rehabilitation procedures.

The S-N approach is widely used to assess the fatigue damage for riveted steel constructions [1-4]. This approach relates the nominal stresses applied on riveted joints with the fatigue life. It requires experimental data for the riveted joint under consideration. This approach shows some limitations such as it suitability only for simple details and loading conditions.

Fracture Mechanics appears as an alternative approach to perform residual life calculations [5,6]. However, the use of the Fracture Mechanics is very often limited to the application of simplified formulae for stress intensity factors evaluation, available in standard handbooks [7]. For example, the stress intensity factor in a cracked plate is calculated by considering an isolated plate rather than a plate integrated in a riveted structural member. No interaction is taken into account between the cracked plate and the remaining components of the member. This may result in inconsistent residual life evaluations, motivating the search for more accurate stress intensity factors evaluation.

Very few works can be found in literature regarding the stress intensity evaluation for riveted built-up beams [8]. Riveted built-up beams are typical from the end of 19th /beginning of 20th centuries, when technology did not offer manufactured hot rolled beams nor welding techniques for making welded connections. Moreno and Valiente [8] proposed an analytical model to assess the stress intensity factors for cracked webs of riveted T beams. The proposed analytical model neglects friction effects and clamping stresses on rivets and is limited to the specific investigated geometry.

Despite numerical procedures (e.g. finite element method plus virtual crack closure technique [9]) have been intensively applied in the assessment of stress intensity factors for structural components and/or joints, they have been disregarded for riveted connections from old riveted bridges.

In a few number of cases, detailed 3D finite element

models have been used in stress analysis of uncracked riveted connections [10-15]. These models have been used to support the application of local stress- and strain-based approaches that requires the evaluation of local/peak stresses of strains for comparison with plain material fatigue strength data, obtained using smooth specimens.

This paper proposes a methodology for detailed stress analysis of multi-riveted connections using the Finite Element Method. The proposed methodology is demonstrated for a stringer-to-cross-girder intersection, using the ANSYS® commercial code [16]. This methodology consists on 3D finite element models, using both solid and shell elements as well as contact elements. The solid elements are used to represent in fine detail the region of interest for the assessment of the local stresses and the shell elements are used elsewhere, aiming a moderate computational cost. Solid-shell interfaces are used to provide required continuity between the shell and solid models. The proposed model is able to account the clamping stresses of rivets on stress distributions. Also, choosing several crack propagation scenarios, the stress intensity factors are evaluated using the crack closure technique [17].

Before the presentation of the multi-rivet joint problem, a single rivet joint is presented to discuss basic issues regarding the finite element analysis of riveted joints.

2. FINITE ELEMENT ANALYSIS OF A SINGLE RIVETED JOINT

A finite element model of a single rivet joint is presented in this section. Figure 1 illustrates the geometry of the riveted joint. This riveted joint was also investigated by Imam et al. [13]. Therefore, it inclusion in this study was the assessment of the proposed procedure. The derived results are compared with existing results available in literature. A discussion is presented regarding the main numerical issues of finite element modelling of riveted joints.

The commercial finite element code ANSYS® [16] was used to analyse the riveted connection. The ANSYS® parametric design language (APDL) was used to build the model of the connection. Both plates and rivet were modelled using 20-node hexahedra solid isoparametric elements (SOLID95).

The contact between the plates and rivet was modelled through contact elements available in ANSYS®, using the surface-to-surface and flexible-to-flexible contact options. In particular, the finite elements CONTA174 and TARGE170 were used to define the several contact pairs [16]. Materials were assumed linear elastic and isotropic (E=210 GPa, ν=0.27). Even assuming linear elastic materials, the finite element analysis still is non-linear due to the contact, which requires an incremental analysis.

Figure 2 shows the finite element mesh of the riveted connection. Only one quarter of the joint was modelled, taking into account the two existing symmetry planes. Displacements at nodes located at planes of symmetry were restrained along the normal direction. Additionally, all degrees of freedom of nodes at face CD (see Figure 1) were restrained. Two types of alternative boundary conditions were tested for face AB: imposed displacement or pressure, applied according the longitudinal or loading direction.

The simulation was carried out using the augmented Lagrange algorithm available in the ANSYS® [16], together with the Coulomb friction model. The augmented Lagrangian method requires the definition of normal contact stiffness. The amount of penetration between the contact and target surfaces depends on the normal stiffness. Higher stiffness values decrease the amount of penetration, but can lead to ill-conditioning of the global stiffness matrix and to convergence difficulties. Lower stiffness values can lead to a certain amount of penetration and produce an inaccurate solution. Ideally, it is desirable a high enough stiffness that the penetration is acceptably small, but a low enough stiffness that the problem will be well-behaved in terms of convergence. In effect, a stiffness relationship between two bodies must be established for contact to occur. Without contact stiffness, bodies will pass through one another. The relationship is generated through an 'elastic spring' that is put between the two bodies, where the contact force is equal to the product of the contact stiffness (κ) and the penetration (δ). The amount of penetration (δ), or incompatibility, between the two bodies is therefore dependent of the stiffness (κ). Ideally, there should be no penetration, but this implies that $\kappa=\infty$, which will lead to numerical instabilities. The value of κ, that is computed by ANSYS®, depends on the relative stiffness of the contacting bodies. There is the possibility of scaling κ through the FKN factor, usually called the normal penalty stiffness factor. The usual factor range is from 0.01-1.0, with a default of 1.0. The default value is appropriate for bulk deformation. Present simulations covered FKN values equal to 0.01, 0.1 and 1.0. Another relevant contact parameter to be used in conjunction with the augmented Lagrangian method is FTOLN. FTOLN is a tolerance factor to be applied in the direction of the surface normal. The range for this factor is less than 1.0 (usually less than 0.2), with a default of 0.1, and is based on the depth of the underlying solid element. This factor is used to determine if penetration compatibility is satisfied. Contact compatibility is satisfied if penetration is within an allowable tolerance (FTOLN times the depth of underlying elements). The depth is defined by the average depth of each individual contact element in the pair. If ANSYS® detects any penetration larger than this tolerance, the global solution is still considered unconverged, even though the residual forces and displacement increments have met convergence criteria. FTOLN values equal to 0.01, 0.05

and 0.1 were simulated. For all other contact parameters not mentioned here, default values were adopted [16].

Null clearance between the rivet hole and rivet shoulder was considered, which is characteristic of riveted joints, but not typical on bolt connections. The effect of the clamping stresses on rivets was modelled. The clamping stresses were generated by a preliminary load step consisting of a temperature variation (decreasing temperature) applied exclusively to the rivet, and assuming orthotropic thermal expansion properties for the rivet: non-null expansion coefficient according the rivet axial direction ($\alpha_z=10^{-5}$ $^oC^{-1}$) and null expansion coefficients according the transverse directions ($\alpha_x=\alpha_y=0$ $^oC^{-1}$). Despite inspired on the riveting process, the application of a temperature change to the rivet was only used as an analytical methodology to generate clamping stresses. The actual clamping stresses on rivets of existing connections are not easy to quantify. Therefore, the proposed model was used to perform sensitivity analysis, seeking the effects of several clamping stresses on the stress distributions around the rivet hole. When clamping stresses are present, the friction effects play a relevant role on stress distributions. In order to illustrate this effect three distinct friction scenarios were investigated: frictionless contact and non-null friction coefficients - μ=0.3 and μ=0.6. The precise value of the friction coefficients is also very difficult to estimate. The friction coefficients tested in this study seems to be plausible values for steel-to-steel contact. Furthermore, μ=0.3 has already been used in literature to simulate the friction effects on riveted connections [13]; μ=0.6 seems to be an upper limit for steel-to-steel contact. When compared with high strength bolts, the clamping stresses on rivets are not significant and not controllable.

A parametric study, illustrating the effects of FKN, FTOLN, μ, clamping stresses and loading conditions was conducted for the single rivet connection, based on 248 simulations. Half of these simulations were carried out for an imposed displacement, δ=0.1 mm, applied to the face AB (see Figure 1) according the longitudinal direction; the other half of the simulations were performed for a pressure p=30 MPa applied to the referred face. For each combination of FKN and FTOLN parameters, 7 distinct clamping stresses were simulated, corresponding to the following temperature variations: 0, 25, 75, 125, 175, 225 and 275 ^{o}C. The simulations carried out for an imposed pressure showed some convergence difficulties for frictionless contact and null clamping stresses.

Figure 3 shows the variation of the average clamping stresses on rivet as a function of the temperature range applied to the rivet. From Figure 3 it is clear that FKN parameter has a significant influence on the clamping stress. The slope of the clamping stress vs. ΔT relation increases with the FKN factor. Friction and FTOLN parameter has a negligible effect on the clamping stress.

Figure 4 illustrates the evolution of the stress intensity as a function of the clamping stress on rivet. The stress intensity was computed dividing the maximum stress on the surface of the hole of the rivet at the central plate, along the loading direction, and the net stress evaluated at the resisting cross section (=remote cross section – projected area of the hole of the rivet). From Figure 4 it is possible to realize that the loading condition (displacement of pressure control) has an effect on stress concentration factor. This may is justified by the friction effect that makes the problem loading path dependent (non-linear).

The stress concentration factor, in the absence of any clamping stress, assumes a value in the range 3-3.5. It is observed that for FKN=1.0, the stress concentration at the rivet hole tends to fade; it can be even lower than unity which means that load transfer is made essentially by friction between the plates. FKN values in the range 1.0-0.1 are plausible, since they produce physically consistent stress intensity evolutions with the clamping stresses. For simulations carried out under displacement control, FTOLN variations within the range 0.1-0.01 did not influence the results. Situation changes if a remote pressure is imposed to the connection - some influence of FTOLN on results is verified.

Table 1 summarizes the stress concentration factors at three distinct locations, namely at the surface of the hole of the side plate (point F – external surface and point G – internal surface/interface) and at the surface of the hole of the middle plate (point H – external surface/interface). These points are located at the plane that contains the rivet axis and is perpendicular to the loading direction. Table 1 also presents stress concentration values obtained at references [13,18] using numerical methods. Deviations between 13% and 40% were verified. Results from reference [18] were computed assuming 2D stress analysis and accounting contact between rivet and the hole using a pressure applied at the hole. Results from reference [13] were obtained from a similar finite element model built in ABAQUS®.

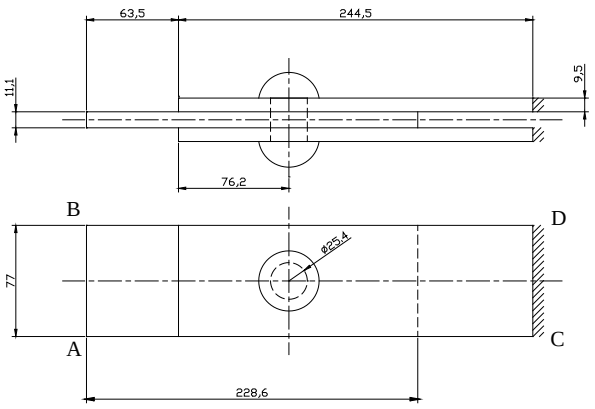

Figure 1. Single rivet joint (dimensions in mm).

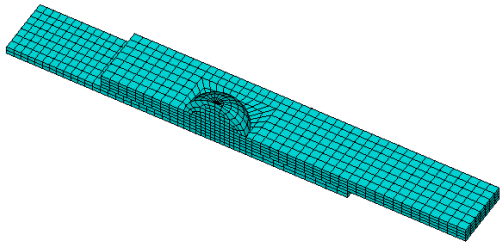

Figure 2. Finite element mesh of a single rivet joint.

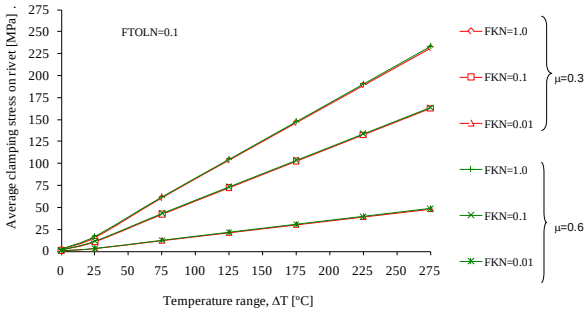

Figure 3. Average clamping stress vs temperature range - single rivet joint.

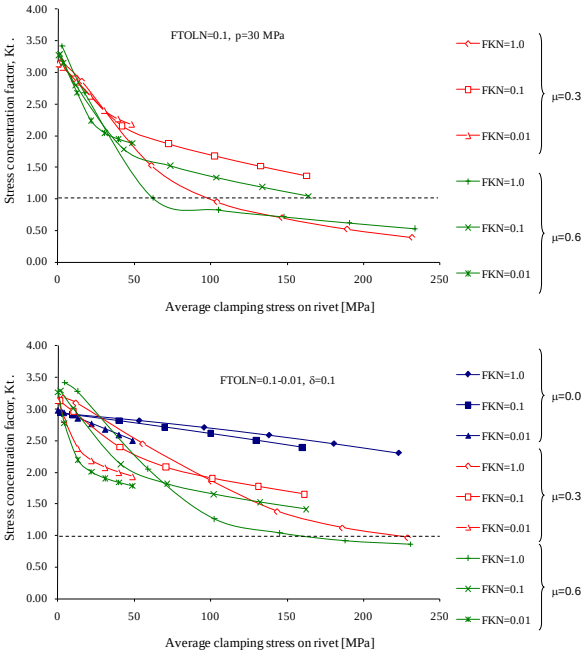

Figure 4. Stress concentration factor vs average clamping stress on rivet - single rivet joint.

Table 1. Stress concentration factor, Kt, for the single rivet joint.

	Locations	F	G	H
This study, FTOLN=0.1-0.01	FKN=1.0	2.70	2.96	2.95
	FKN=0.1	2.67	2.86	3.13
	FKN=0.01	2.81	2.87	3.14
	Average	2.73	2.90	3.07
[11]		2.19	2.19	2.17
[8]		1.97	1.75	2.68
[11] - Deviation (%)		19.6	24.2	29.2
[8] - Deviation (%)		27.8	39.7	12.7

3. FINITE ELEMENT ANALYSIS OF A STRINGER-TO-CROSS-GIRDER JOINT

This section presents the results of a finite element model of a riveted structure, namely composed of one cross girder connected to two stringers, by means of rivets. Both members are I shape beams and the connection is established by means of angles and rivets, attaching the webs of the beams. Figure 5 shows the global geometry of the beam and Figure 6 the finite element mesh. Only ¼ of the geometry was modelled taking into account existing planes of symmetry. The finite element model is composed of 3D solid elements (SOLID95) at joint location and shell elements (SHELL93) elsewhere [16]. The two types of elements are attached using contact element technology [16]. Simulations were carried with default contact parameters (FKN=1.0, FTOLN=0.1), since previous section demonstrated to yield consistent results. Furthermore, it was assumed: μ=0.3, E=210 GPa and ν=0.3. The clamping stresses on rivets were modelled through a temperature variation, as proposed in the previous section. Roughly, a linear approximation was verified between the clamping stresses and the temperature range. Figure 7 shows the vertical (P direction) displacement field. It is verified that a smooth transition is obtained at solid-shell interface, which is a good indication of the quality of the results.

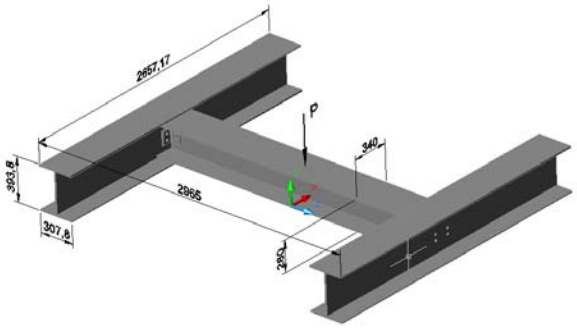

Figure 5. Riveted structure: stringer-to-cross-girder intersection (dimension in mm, P=200kN).

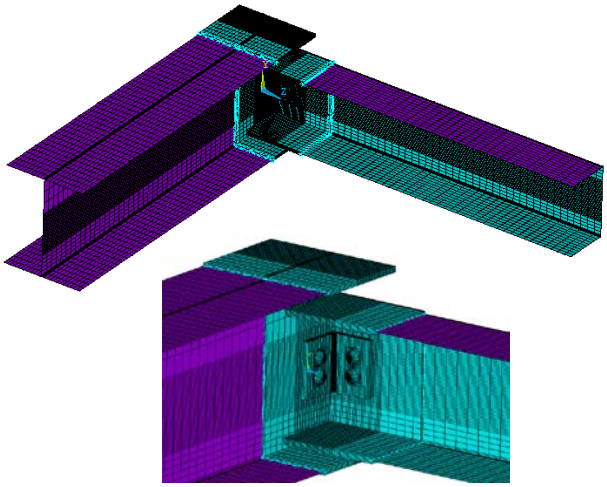

Figure 6. FE mesh of the stringer-to-cross-girder intersection.

Figure 8 shows the evolution of the maximum deflection in the cross girder, as a function of the clamping stresses (temperature range) and friction. Consistent results were derived: deflection decreases with the increasing of the clamping stresses and friction. Figure 9 illustrates the stress fields at the end of the web of the cross girder. It is verified two critical locations that may lead to crack initiation. Figure 10 shows the stress concentration evolution with clamping stresses on rivets and friction. This stress concentration was evaluated dividing the maximum stress around the rivet holes (see Figure 9) by the maximum theoretical bending stress at the end of the girder. There is a stress concentration reduction as the clamping stress and friction effects increases. Three crack propagation scenarios were investigated. Figure 11 illustrates the stress fields for representative cracks emanating from the rivet holes at the web of the girder.

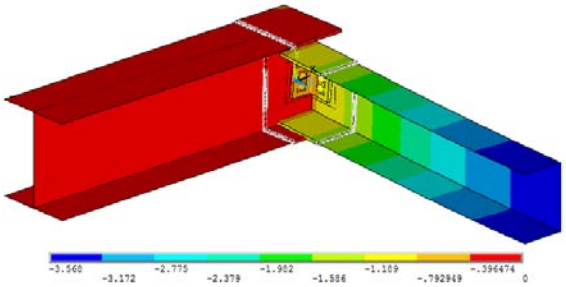

Figure 7. Stringer-to-cross-girder intersection: vertical displacement field, u_y, mm ($\Delta T=0^oC$).

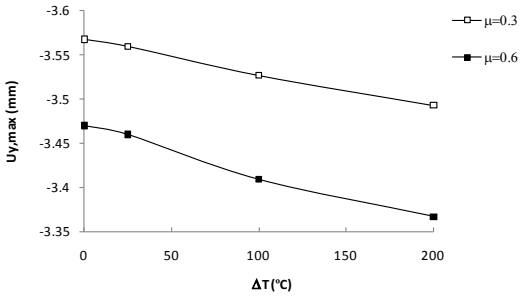

Figure 8. Stringer-to-cross-girder intersection: maximum vertical displacement at cross girder.

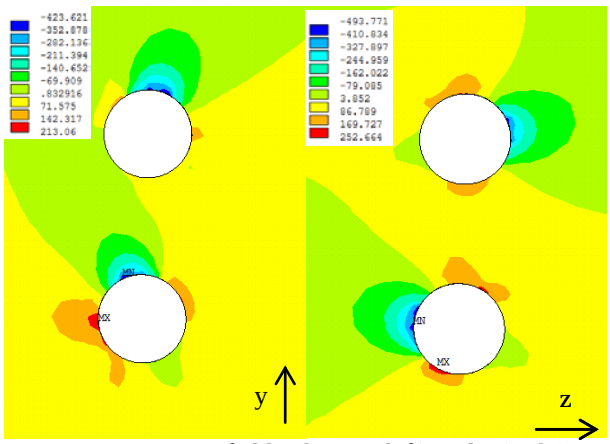

Figure 9. Stress fields along y (left) and z (right) directions at the riveted end of the cross girder.

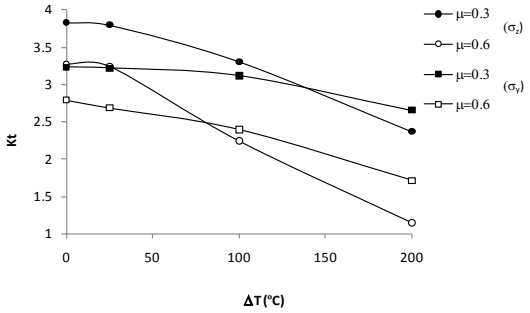

Figure 10. Stress concentration factors around rivet holes of the girder.

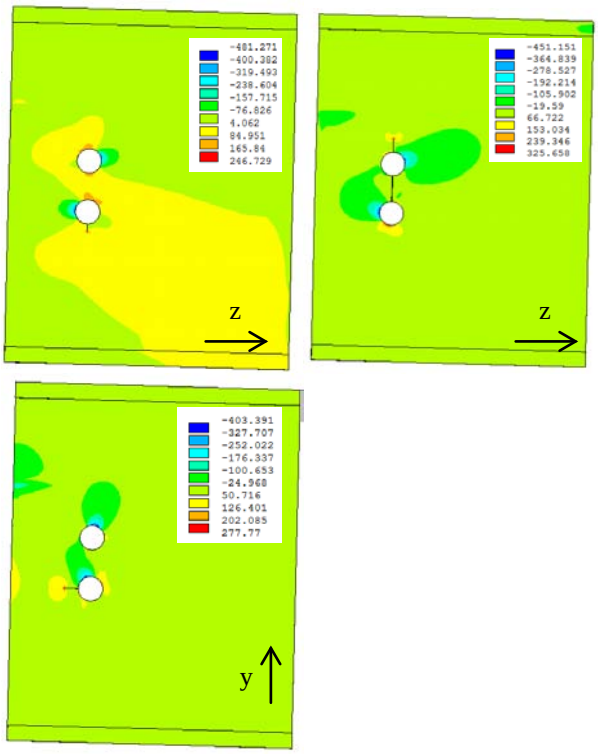

Figure 11. Stress fields along z (top) and y (bottom) directions for the cracked end of the cross girder.

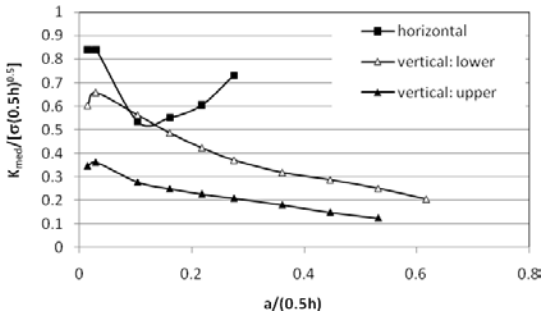

Figure 12. Stress intensity factors for the several crack propagation scenarios. (h: height of the girder; σ: maximum bending stress on girder from beam bending theory)

Figure 12 shows the stress intensity evolution for the three crack propagation scenarios. The stress intensity factors were computed using the crack closure method in two analysis steps as well the virtual crack close technique [17]. Results shown in Figure 12 are averaged

results through the web thickness, and normalized using the maximum theoretical bending stress for a fixed-fixed beam under central point load. The scenario of a horizontal propagating crack seems to be the most critical one, since the stress intensity factor is always higher than values computed for the other cracks. Stress intensity factors for the vertical cracks tends to decrease as the crack growths, therefore any vertical fatigue crack tends to slow down.

4. CONCLUDING REMARKS

A methodology for detailed stress analysis of multi-riveted connections using the Finite Element Method was proposed, using the ANSYS® commercial code. The proposed methodology is demonstrated for a stringer-to-cross-girder intersection. This methodology consists on 3D finite element models using both solid and shell elements as well as contact elements. The proposed model is able to account the clamping stresses of rivets as well as friction on stress distributions. Also, choosing several crack propagation scenarios, the stress intensity factors are evaluated using the crack closure technique. A comparison between the stress intensity factors allows the assessment of the most critical scenarios, from a fatigue perspective.

ACKNOWLEDGEMENTS

The authors acknowledge the Portuguese Science Foundation for the support through the research project PTDC/EME-PME/78833/2006.

REFERENCES

[1] DiBattista, J.D., Adamson D.E.J. and Kulak G.L., "Evaluation of remaining fatigue life for riveted truss bridges", *Canadian Journal of Civil Engineering*, 25(4), pag. 678-691, 1998.

[2] Geissler, K., "Assessment of old steel bridges, Germany", *Structural Engineering International*, 12(4), pag. 258-263, 2002.

[3] Kulak, G.L., "Fatigue strength of riveted shear splices", *Progress in Structural Engineering and Materials*, 2(1), pag. 110-119, 2000.

[4] Kim, S.-H., Lee, S.-W., Mha, H.-S. "Fatigue reliability assessment of an existing steel railroad bridge", *Engineering Structures*, 23, pag. 1203-1211, 2001.

[5] Wang, C.S., Chen, A.R., Chen, W.Z., Xu, Y., "Application of probabilistic fracture mechanics in evaluation of existing riveted bridges", *Bridge Structures*, 2(4), pag. 223-232, 2006.

[6] Paasch, R.K., DePiero, A.H., *Fatigue Crack Modeling in Bridge Deck Connection Details*, Final Report SPR 380, Oregon Department of Transportation, 1999.

[7] Tada, H., Paris. P.C., Irwin, G.R., *The stress analysis of cracks handbook*, ASME Press, 2000.

[8] Moreno, J., Valiente, A., "Stress intensity factors in riveted steel beams", *Engineering Failure Analysis*, 11, pag. 777-787, 2004.

[9] Rijck, J.J.M., *Stress Analysis of Fatigue Cracks in Mechanically Fastened Joints. An analytical and experimental investigation*, Ph.D. Thesis, 302 pag., Delft, The Netherlands, 2005.

[10] DePiero, A.H., Paasch, R.K., Lovejoy, S.C., "Finite-element modeling of bridge deck connections details", *Journal of Bridge Engineering*, 7(4), pag. 229-235, 2002.

[11] Al-Emrani, M., Kliger, R., "FE analysis of stringer-to-floor beam connections in riveted railway bridges", *Journal of Constructional Steel Research* 59(7), pag.803-818, 2003.

[12] Iman, B., *Fatigue analysis of riveted railway bridges*. Ph.D. Thesis, 258 pag., School of Engineering, University of Surrey, UK, 2006.

[13] Imam, B.M., Righiniotis, T.D., Chryssanthopoulos, M.K., "Numerical modelling of riveted railway bridge connections for fatigue evaluation", *Engineering Structures*, 29, pag. 3071-3081, 2007.

[14] Righiniotis, T.D., Imam, B.M., Chryssanthopoulos, M.K., "Fatigue analysis of riveted railway bridge connections using the theory of critical distances", *Engineering Structures*, 30, pag. 2707-2715, 2008.

[15] De Jesus, A.M.P., Pinto, H., Fernández-Canteli, A., Castillo, E., Correia, J.A.F.O., "Fatigue assessment of a riveted shear splice based on a probabilistic model", *International Journal of Fatigue*, 32, pag. 453-462, 2010.

[16] SAS - Swanson Analysis Systems Inc., ANSYS, Version 11.0, Houston, 2009.

[17] Krueger, R., "Virtual crack closure technique: History, approach, and applications", *Applied Mechanics Reviews*, 57(2), pag. 109-143, 2004.

[18] Shivakumar, K.N., Newman, J.C., "Stress concentrations for straight-shank and countersunk holes in plates subjected to tension, bending and pin loading", NASA Technical Paper No. 3192, 1992.